J Mater Sci (2008) 43:5441–5447
DOI 10.1007/s10853-008-2844-2

# The permeability of Lost Foam pattern coatings for Al alloy castings

**W. D. Griffiths · P. J. Davies**

Received: 20 December 2007 / Accepted: 27 June 2008 / Published online: 18 July 2008


**Abstract** The Lost Foam casting of Al alloys has not yet reached its full potential because of the complexity of the process, and the fact that it is still poorly understood. In this paper, the permeability of typical pattern coatings for the Lost Foam casting of Al was measured, and found to vary from about 0.1 Darcy, ($10^{-13}$ $m^2$), for a low permeability coating, to about 1 Darcy ($10^{-12}$ $m^2$), for a high permeability coating. Permeability was reduced by increasing coating thickness, but examination of the coatings on a hot-stage SEM suggested it would be unaffected by increased temperature. The results were used to infer how the filling of a Lost Foam polystyrene pattern could be influenced by the permeability of the pattern coating.

## Introduction

The Lost Foam or evaporative pattern casting process has the potential to be used for extremely complex castings, which are not easily manufactured by conventional casting processes. However, while offering economic advantages, Lost Foam casting is associated with very high failure rates because of a lack of understanding of the fundamental mechanisms involved in the process, and a lack of knowledge as to how the process variables should be controlled in order to achieve high quality castings.

The Lost Foam casting process uses a pattern formed from expanded polystyrene (EPS), which is dipped in a water-based refractory slurry to provide a thin coating of around 0.5-mm-thickness. After drying, the coated pattern is placed in a moulding box that is filled with loose dry sand, which is compacted by vibration to form a rigid mould to support the pattern. The mould is then filled with liquid metal, with the polystyrene pattern left in place, where it is degraded by the heat of the cast metal.

The coating allows the retention of the shape of the mould cavity in the gap between the receding degradation front of the pattern and the advancing liquid metal filling the mould. Secondly, because it is permeable, the degradation products of the pattern can pass through it. It has been proposed that, in the case of an aluminium casting, the polystyrene pattern degrades first to short molecular chain liquids and liquid styrene, which may be absorbed into the permeable coating, and then subsequently to vapour by-products including styrene vapour, water vapour and carbon dioxide, which pass through the permeable coating into the surrounding sand [1]. The pattern coatings usually consist of water-based slurries that contain refractory particles such as alumina, silica and mica, and binders, such as polyvinyl acetate, dextrines and acrylics, together with dispersants, suspension agents and biocides [2].

In previous work, pattern coating permeability has been measured using a disc of coating clamped between two silicone gaskets with air forced through the coating at a controlled pressure (typically between 7 and 20 kPa) [3]. Airflow rates and the pressure differences across the coated discs were measured and Darcy's law for the permeability of a porous medium (see Eq. 1) [4–7] used to calculate the permeability of the coatings. Forchheimer's equation [8]

W. D. Griffiths (✉)
Department of Metallurgy and Materials Science, School of Engineering, University of Birmingham, Edgbaston, Birmingham B15 2TT, UK
e-mail: W.D.Griffiths@bham.ac.uk

P. J. Davies
Honda of the UK Manufacturing Ltd., Highworth Road, South Marston, Swindon, Wiltshire SN3 4TZ, UK

has been shown to give more reliable information than Darcy's law on the permeability of highly porous structures where fluid velocities are high (such as in ceramic foam filters used in metal filtration), but Darcy's law has been considered to be valid in the case of Lost Foam coatings due to the low velocity of the fluid flow in the coatings [9, 10].

For laminar viscous flow through a macroscopically homogeneous porous material, Darcy's law states [4]

$$\frac{\Delta P}{L} = \frac{\mu}{k_1} U \tag{1}$$

where $\Delta P$ is the total pressure drop across a medium of thickness $L$ and specific permeability $k_1$. $U$ is the superficial velocity of the fluid, with dynamic viscosity $\mu$, and is considered uniform in the medium [4];

$$U = \frac{\Delta Q}{A} \tag{2}$$

where $\Delta Q$ is the measured flow rate through the medium and $A$ is the cross-sectional area [5].

A number of researchers [3, 10, 11] have used different methods to measure the permeability of various pattern coatings, but unfortunately few values have been published. Instead coatings have been generally characterised as having "high" or "low" permeability, and this has made it difficult to make comparisons between the results of casting experiments of different researchers. Furthermore, conventional empty cavity casting processes have benefited greatly from computer simulation. But the modelling of Lost Foam casting is not at the same level of capability, partly because the process is more complicated, and partly because many of the mechanisms involved are not well understood. For these reasons it is important to understand, quantitatively, the permeability of the pattern coating and its role in allowing the removal of gaseous pattern degradation products, and the formation of gas entrapment defects. The results reported here are aimed at providing basic data for the permeability of pattern coatings used in the Lost Foam casting of Al alloys, to aid in understanding the casting process, and to facilitate its mathematical modelling.

## Experimental procedure

Samples of pattern coatings for permeability measurement were produced by applying the coating material to a supporting mesh, made from 0.112 mm diameter stainless steel wire, with 100 wires per 25 mm, cut into 40 mm diameter discs. Coating thicknesses of between 300 and 600 μm were tested (typical of pattern coatings used in practice), with either three or six samples made and tested for each thickness. Once coated, the disc samples were dried at a temperature of 125 ± 2 °C for 10 min. (It was not possible to directly measure the permeability of coating samples removed from patterns because of their fragility.)

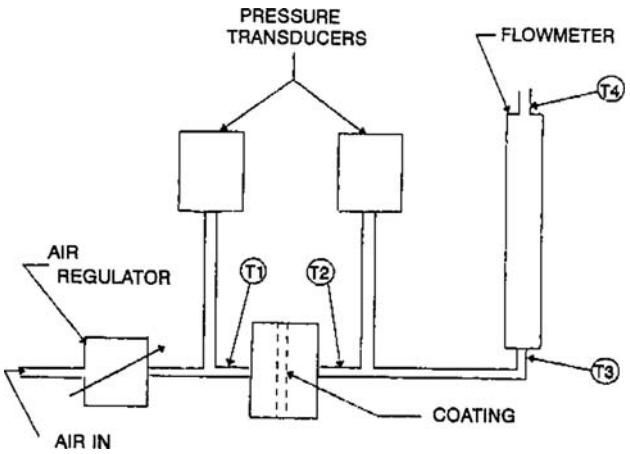


**Fig. 1** Sketch of equipment used to measure coating permeability (after [3])

The equipment used to measure airflow through the coating samples was based on the apparatus developed by Littleton et al. [3] and has been shown in Fig. 1. The coated discs were clamped into a sample holder made from two aluminium discs bolted together. The sample holder (complete with the coated disc) was placed in a chamber split into two halves, each half having an O-ring that formed an airtight seal on the sample holder when the chamber was screwed together.

Compressed air was forced through the chamber and hence through the coating sample at a pressure of between 0.1 and 0.2 MPa, controlled by a pressure regulator. The pressure difference across the coating was recorded by pressure transducers placed at either side, connected to a PC-based data acquisition system. A flowmeter was used to measure the rates of airflow through the coating samples, and the resulting data was used in Eq. 1 to calculate the permeability, $k_1$, of each coating. The equipment was tested by sealing the surfaces of a coating sample with wax and placing the apparatus under pressure, to demonstrate that the equipment did not leak.

The permeability values of three commercial Lost Foam coatings for Al castings (supplied by Foseco Morval, Ontario, Canada) were measured. The compositions of the coatings were predominantly mica in a water carrier, with binders, anti-foaming agents, wetting agents and biocides. Four dilutions of each of the three different coating grades were produced to obtain coating samples with four different thicknesses. The effective cross-sectional area of the coated mesh sample was obtained by subtracting the area occupied by the wires in the mesh from the total area of the coating, and was $3.11 \times 10^{-4}$ m$^2$.

A JEOL 6060 scanning electron microscope (SEM) was used to examine the internal and surface structure of each of the coating types. For this purpose, 10 mm × 10 mm samples of coatings were carefully removed from coated EPS patterns using a scalpel and mounted using standard methods.

It was thought that alterations in the coating structure and hence its permeability might occur as they became heated, so coating samples were placed in a Phillips XL-30 Field Emission Gun environmental scanning electron microscope (FEG-SEM), equipped with a hot-stage apparatus, to observe the coating samples as they were heated at a rate of 30 K $min^{-1}$, to a maximum temperature of approximately 700 °C. The coating samples were of size 2.5 mm × 2.5 mm × 500 μm, and were cut from coated EPS patterns using a scalpel and mounted vertically onto stainless steel mesh using a small amount of coating slurry as an adhesive.

## Results

Figure 2 shows the change in permeability with coating thickness for the three mica-based pattern coatings examined. Each data point has been shown, and it can be seen that the reproducibility of the measured permeability of the samples with similar thickness was good. The permeability results are also shown in Table 1, together with their standard deviations. For a coating thickness of about 0.33 mm, the low permeability coating had a mean permeability of about $9.5 \times 10^{-14}$ $m^2$, the medium permeability coating had a mean value of about $1.8 \times 10^{-13}$ $m^2$, and the high permeability coating had a mean value of about $9 \times 10^{-13}$ $m^2$ (determined by interpolation), a range that was about an order of magnitude. The measured permeability decreased with increased coating thickness. For example, with nearly double the thickness, 0.6 mm, values of about $7.1 \times 10^{-14}$ $m^2$ and $4.3 \times 10^{-13}$ $m^2$ were obtained for the low and high permeability coatings, a decrease of about one-quarter and one-half, respectively. The measurement error in these values was estimated to be <5% (determined from the error in the measurement of the coating thickness, pressure, and airflow rate).

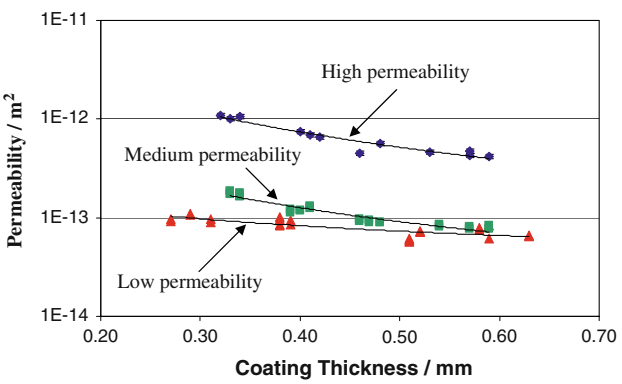


**Fig. 2** Measured permeability values of the three Lost Foam pattern coatings, for a range of coating thicknesses

Figure 3 shows the internal structure of a coating, obtained by fracturing a portion of coating removed from a pattern. This showed flat, aligned, mica particles, parallel to the foam pattern surface, with smaller particles filling the voids between the larger mica plates. This image is from the high permeability coating, but the other coatings appeared similar.

Particle sizes were determined from coating images, and from data obtained from the coating supplier, Foseco Morval, Ontario, Canada. The low permeability coating comprised mainly small mica particles of between 10 and 30 μm in diameter, which appeared to pack together closely (see Fig. 4a). This structure would result in fewer flow paths and explained the low permeability of this coating. Conversely, the high permeability coating contained larger mica particles of between 70 and 100 μm, which packed together less closely (see Fig. 4c) and therefore provided much less resistance to flow, giving higher permeability. The medium permeability coating was composed of intermediate sized particles of between 20 and 50 μm (see Fig. 4b).

The surface of the low permeability coating adjacent to the pattern is shown in Fig. 5a. This contained many pores of an average diameter of about 30 μm, although no evidence could be found that these pores extended through the thickness of the coating. The surfaces of the other coatings were more uniform, and there were no obvious signs of any pores that may have contributed to their permeability (see Fig. 5b, c). (A 150 μm diameter pore was observed in the surface of the coating in Fig. 5c, but this was an isolated occurrence.)

Figure 6 shows a cross section of a sample of coating (of low permeability), which had been removed from an EPS pattern and had a small piece of the pattern attached. The pattern surface was observed to be in good contact with the refractory coating, and coating material had penetrated the interstices between the EPS beads nearest the pattern surface. This resulted in a coating surface with peaks corresponding to the bead spacing, often replicated on the casting surface.

When coating samples were heated from room temperature to about 700 °C, the spaces between individual particles appeared to increase with temperature. For example, Fig. 7 shows a cut surface of a sample of the medium permeability coating at temperatures of about 150 °C (Fig. 7a) and about 700 °C (Fig. 7b). The coating structure appeared to have become more open when the

**Table 1** Summary of the coating permeability measurements

| Type of coating | Mean sample thickness (mm) | Number of samples | Mean permeability ($m^2$) | Standard deviation ($m^2$) |
|---|---|---|---|---|
| Low permeability | 0.29 | 6 | $9.8 \times 10^{-14}$ | $7.4 \times 10^{-15}$ |
| | 0.38 | 6 | $9.1 \times 10^{-14}$ | $7.3 \times 10^{-15}$ |
| | 0.51 | 6 | $6.4 \times 10^{-14}$ | $6.6 \times 10^{-15}$ |
| | 0.60 | 6 | $7.2 \times 10^{-14}$ | $9.3 \times 10^{-15}$ |
| Medium permeability | 0.34 | 6 | $1.7 \times 10^{-13}$ | $7.8 \times 10^{-15}$ |
| | 0.40 | 6 | $1.2 \times 10^{-13}$ | $5.9 \times 10^{-15}$ |
| | 0.47 | 6 | $9.2 \times 10^{-14}$ | $3.0 \times 10^{-15}$ |
| | 0.57 | 6 | $8.1 \times 10^{-14}$ | $3.3 \times 10^{-15}$ |
| High permeability | 0.33 | 3 | $9.0 \times 10^{-13}$ | $2.1 \times 10^{-13}$ |
| | 0.41 | 3 | $7.0 \times 10^{-13}$ | $5.2 \times 10^{-14}$ |
| | 0.49 | 3 | $4.9 \times 10^{-13}$ | $6.5 \times 10^{-14}$ |
| | 0.58 | 3 | $4.4 \times 10^{-13}$ | $3.0 \times 10^{-14}$ |

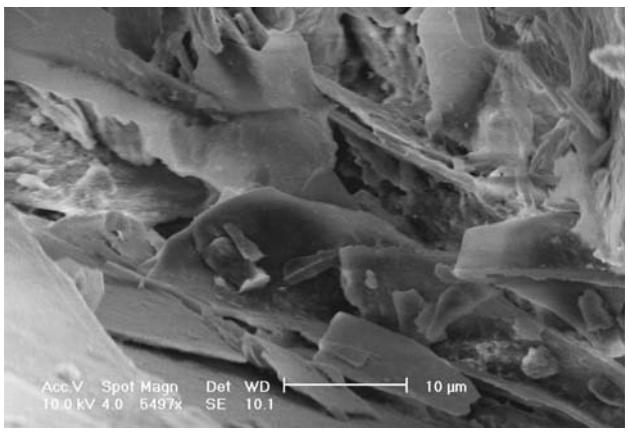


**Fig. 3** SEM image showing the arrangement of the mica particles in the high permeability coating. The plate-like particles were aligned parallel to one another, with smaller particles of mica and other refractory materials in between

temperature was increased, but the measured distances between the two particles A and B in Fig. 7 had not changed, suggesting any change in coating structure was minimal. It was inferred that any changes in appearance were probably due to the straightening of mica particles that had become folded over when the samples were cut from the patterns, but which straightened upon heating.

## Discussion

Permeability is described in units of Darcy, (D), and 1 Darcy = $10^{-12}$ $m^2$; therefore, from these measurements, the low permeability coating had a permeability of about 0.1 D, and the high permeability coating about 1 D. The measured permeability values obtained were slightly greater than those found by other workers, which were reported to be about 0.05–0.1 D [12] and $1 \times 10^{-10}$ to $1 \times 10^{-9}$ $cm^2$ (or 0.01–0.1 D) (H. Littleton, personal communication).

The measured values of each coating correlated well with the appearance of the coatings as revealed by SEM examination; the lowest permeability values were for the coating containing the smaller particles, where the particles would pack together more closely than would larger particles, giving a structure that provided more resistance to gas flow.

The permeability of each coating was found to decrease when coating thickness was increased, as had been earlier observed [2, 13]. This was probably mainly due to the increase in thickness, but may also be related to the different coating slurry viscosities that were used to produce the range of coating thickness. (It was necessary to dilute the original coating slurries with water, reducing their viscosity, in order to obtain thinner coating samples; consequently, the size and size distribution of the refractory particles adhering to the mesh discs after dipping may not have been constant.) The coatings had similar structures, aligned plate-like particles (see Fig. 4), but with variations in particle size. The pores observed in Fig. 5 did not pass through the coatings, and should not have influenced their porosity greatly. It therefore seems that quite large changes in particle size are necessary to influence permeability, and that changing coating thickness did not have a great effect.

It was considered possible that the coating structure may become more open, and therefore more permeable, as it is heated during mould filling. Consequently, coating permeability measurements that are made at room temperature may not accurately represent the permeability of the coating in the mould when the casting is actually being filled. However, the hot-stage SEM examinations did not suggest changes in coating structure that would influence

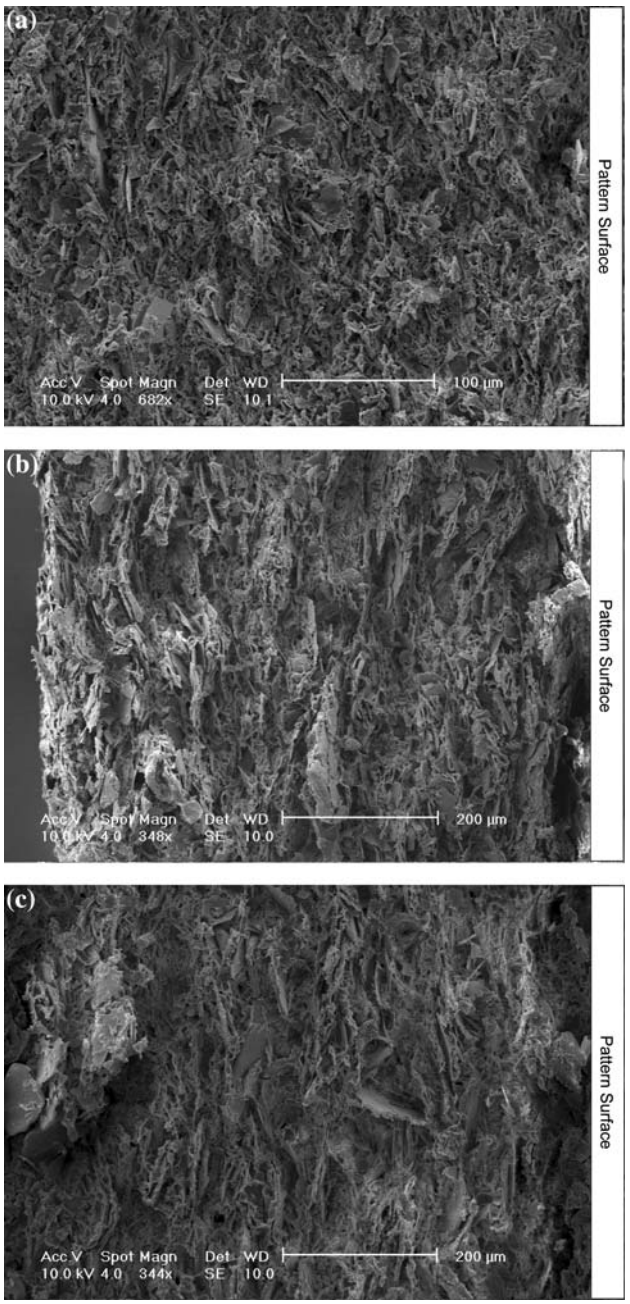


**Fig. 4** (**a**) SEM image showing the internal structure of a low permeability coating; average particle size = 10–30 μm. (The scale bar in this image is 100 μm, while in (**b**) and (**c**) the scale bar is 200 μm). (**b**) SEM image showing the internal structure of a coating of medium permeability; average particle size = 20–50 μm. (**c**) SEM image showing the internal structure of a high permeability coating; average particle size = 70–100 μm

coating permeability, and therefore measurements of coating permeability obtained at room temperature should still be valid at the temperature of the coating in the casting process.

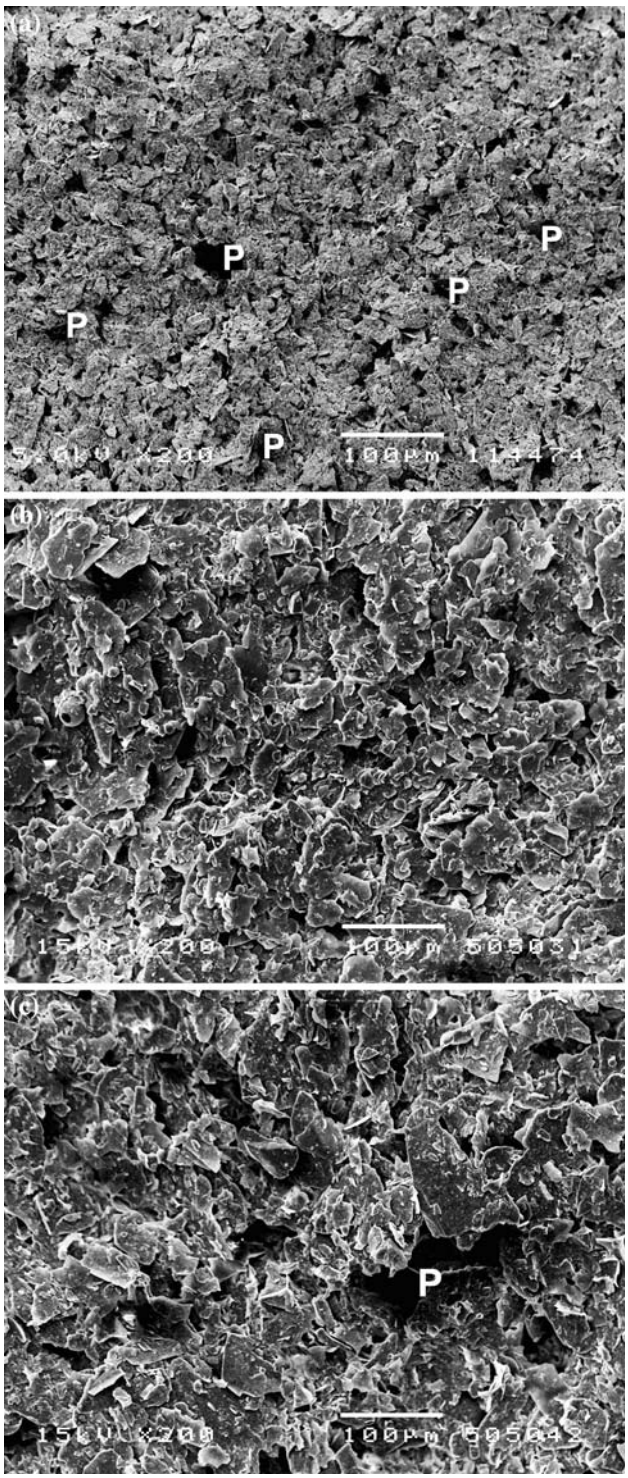


**Fig. 5** (**a**) SEM image of the pattern-bonding surface of a coating of low permeability. The surface contained many pores (labelled P) of average diameter 30 μm. (**b**) SEM image of the pattern-bonding surface of a coating of medium permeability. Few pores were observed in the coating surface. (**c**) SEM image of the pattern-bonding surface of a high permeability coating. P indicates a large pore

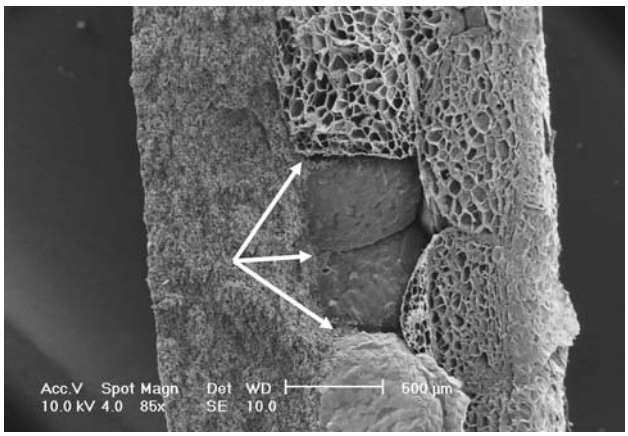


**Fig. 6** SEM image of a cross section of a low permeability coating with attached EPS pattern material. Arrows indicate where the coating had filled the voids between adjoining foam beads

The rate of gas flow through a permeable material can be calculated using Eqs. 1 and 2. Topologically, a thin plate pattern is similar to the types of castings often produced in the Lost Foam casting process, such as casings for components; it is useful to consider the degradation of a thin plate of EPS in order to illustrate the role of the pattern coating in the process.

An EPS plate pattern of size, length = 0.5 m, width = 0.25 m and thickness = 0.01 m would have a volume of 0.00125 $m^3$ (1,250 $cm^3$) and surface area of 0.265 $m^2$. The gas contained within this pattern, which must pass through the coating, would be this volume of air plus the volume of gaseous degradation products from the pattern. The volume of gas evolved from EPS has been determined to be 216 $cm^3$ of gas, for 1 g of polymer, if it was completely transformed to styrene monomer [14]. But in the casting of Al, the amount of gaseous degradation products produced has been estimated to be only 6 to 30%, the remainder being liquid degradation products [14]. A typical density for an expanded polystyrene (EPS) pattern would be about 25 kg $m^{-3}$ (0.025 g $cm^{-3}$) and the rectangular pattern considered would have a mass of 31.25 g. Its coating has to allow for the passage of the gas contained in the pattern (1,250 $cm^3$) and the gas evolved during pattern degradation. Assuming 20% of the mass of the pattern breaks down to a gas (6.25 g), this would have a volume of 1,350 $cm^3$, giving a total gas volume of 2,600 $cm^3$.

A typical pattern coating thickness would be about 0.5 mm. The pressure inside a pattern during filling with Al has been measured to be about 200–500 Pa [15]. Table 2 shows calculated gas flow rates, for the high and low permeability coatings examined here, assuming atmospheric pressure external to the pattern, an excess pressure inside the pattern of 500 Pa, and that the gas passing through the coating has the viscosity of air (about $4 \times 10^{-5}$ Pas at 700 °C). The gas flow rates per $cm^2$ would range from about 0.25 $cm^3$ $cm^{-2}$ $s^{-1}$ for the low permeability coating to about 2.5 $cm^3$ $cm^{-2}$ $s^{-1}$ for the high permeability coating.

A rate of vaporisation of EPS of 0.015 g $cm^{-2}$ $s^{-1}$ has been estimated from casting experiments (where the area referred to is the area of the liquid metal–EPS pattern interface) [14]. For a liquid Al front advancing through the plate pattern described earlier, with a velocity of 1 cm $s^{-1}$, the metal front would sweep through a volume of 25 $cm^3$ in 1 s, generating from the degrading foam a volume of 27 $cm^3$ of gas (again assuming 20% of the foam became vaporised and 80% became liquid). With the displaced air this is a total of 52 $cm^3$ of gas produced each second, which should pass through the coating. The area of the

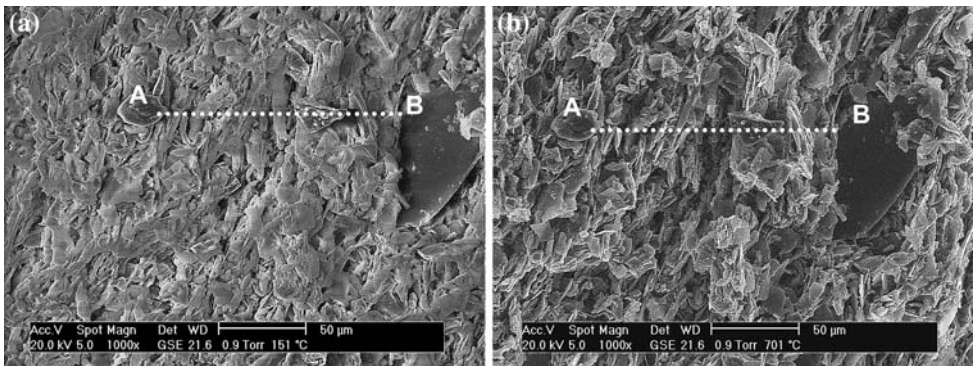


**Fig. 7** SEM micrographs of a pattern coating at a temperature of (**a**) about 150 °C and (**b**) after heating to about 700 °C

**Table 2** Estimated gas flow rates through pattern coatings

| Coating permeability | Permeability ($m^2$) | Gas flow rate through coating ($cm^3$ $s^{-1}$) | Gas flow rate ($cm^3$ $s^{-1}$ $cm^{-2}$) |
|---|---|---|---|
| Low | $1 \times 10^{-13}$ | 663 | 0.25 |
| High | $1 \times 10^{-12}$ | 6,630 | 2.5 |

coating, for the swept volume considered, is 52 $cm^2$, and therefore the permeability of the pattern coating must be such as to allow 1 $cm^3$ of gas to pass through an area of 1 $cm^2$ per second (i.e. 1 $cm^3$ $cm^{-2}$ $s^{-1}$), in order to prevent gas from the degradation of the pattern from accumulating at the liquid metal–pattern interface.

The observation that the estimated flow rates through the low and high permeability coatings lie above and below this estimated rate of evolution of the gas suggests how the permeability of the coatings might affect the degradation of the pattern and the filling of the mould.

With the low permeability coating, the potential rate of gas flow through the coating ($\sim$0.25 $cm^3$ $cm^{-2}$ $s^{-1}$) was less than the estimated total rate of gas production ($\sim$1 $cm^3$ $cm^{-2}$ $s^{-1}$). In this case, the gas (vapour degradation products + air) would accumulate in the liquid metal–coating interface, causing a reduction in the rate of evolution of vapour, as the heat transfer from the liquid metal to the degrading EPS was reduced by the increase in the gap between the EPS and the liquid metal. As the metal–EPS interface gap increased, a greater area of coating would become available for the accumulated gas to escape through, and the rate of vapour production would decline, both effects leading to a reduction in the distance between the liquid metal and the EPS, increasing heat transfer and increasing gas evolution rates again. This fluctuation in metal–foam interfacial heat transfer caused by accumulation of the vapour degradation products might lead to an unstable advancing liquid metal front and entrapment of gas bubbles and other degradation products in the casting.

With the high permeability coating, the potential rate of gas flow through the coating was greater than the rate of gas production ($\sim$2.5 $cm^3$ $cm^{-2}$ $s^{-1}$compared to 1 $cm^3$ $cm^{-2}$ $s^{-1}$). In this case, the filling of the mould should not be controlled by the balance between vapour production and escape, but by other factors, perhaps by the amount and distribution of liquid degradation product.

It should be borne in mind that these considerations were arrived at by using rates of vaporisation, and estimates of the amount of gaseous degradation products, that are only approximately valid for the Lost Foam casting process in general. The observations also apply only to Al castings; the coatings used in the case of iron castings, for example, have much greater permeability. A more detailed understanding of the process would lead to a better model of how the pattern coating permeability should be controlled in order to improve the casting process.

## Conclusions

1. The permeability of typical coatings used in the Lost Foam process for casting Al alloys has been measured and found to vary from about 0.1 Darcy, ($10^{-13}$ $m^2$), for a low permeability coating, to about 1 Darcy ($10^{-12}$ $m^2$), for a high permeability coating.
2. Examination of the structure of the coatings in a hot-stage FEG-SEM did not suggest any changes in structure that would affect permeability, at temperatures of up to 700 °C. Therefore measurements of coating permeability at room temperature should be valid at temperatures reached in the casting process.
3. Consideration of the rate of degradation of an expanded polystyrene pattern, and the proportion of the degradation product that forms a vapour, suggested that low permeability pattern coatings may be insufficiently permeable to allow the passage of gaseous degradation products at a rate greater than they are generated. This would lead to an accumulation of gases in the liquid metal-foam pattern interface that may, in its turn, affect the rate of degradation of the pattern.
4. The same considerations suggested that a high permeability pattern coating was sufficiently permeable to allow the passage of gaseous degradation products at a rate greater than they would be produced.

**Acknowledgements** The authors would like to gratefully acknowledge the assistance of Mr. Adrian Caden of the University of Birmingham with the execution of the experiments, Mr. Dennis Nolan of Foseco Morval, Ontario, Canada, for provision of materials, and EPSRC for the provision of a studentship for one of the authors (PJD).

## References

1. Shivkumar S, Wang L, Apelian D (1990) JOM 42:38
2. Martinez OA (1990) AFS Trans 98:241
3. Littleton HE, Miller BA, Sheldon D, Bates CE (1996) AFS Trans 104:335
4. Philipse AP, Schram HL (1991) J Am Ceram Soc 74:728. doi: 10.1111/j.1151-2916.1991.tb06916.x
5. Massey BS (1995) Mechanics of fluids. Chapman & Hall, London
6. Darcy H (1856) Les fontaines publiques de la ville de dijon. Victor Dalmont, Paris
7. Liu Y, Bakhtiyarov SI, Overfelt RA (2002) J Math Sci 37:2997. doi:10.1023/A:1016029300243
8. Innocentini MDM, Salvini VR, Pandolfelli VC, Coury JR (1999) J Am Ceram Soc 82:1945
9. Burditt MF (1988) Mod Cast:20
10. Spada AT (2001) Mod Cast:27
11. Kocan GH (1996) AFS Trans 104:565
12. Shivkumar S, Gallois B (1987) AFS Trans 95:801
13. Bex T (1989) Mod Cast:34
14. Shivkumar S, Gallois B (1987) AFS Trans 95:791
15. Yang J, Huang T, Fu J (1998) AFS Trans 106:21